AUTOMATED DETECTION OF BASALT SPECTRA IN CLEMENTINE LUNAR DATA. I. Antonenko and G.R. Osinski, Canadian Lunar Research Network, University of Western Ontario, Department of Earth Sciences, 1115 Richmond St. London, ON N6A 5B7, Canada. iantonenk@uwo.ca.

Introduction: Identifying basalts in surface or subsurface deposits is fundamental for our understanding of the 2D and 3D distribution of volcanic rocks on the Moon. For example, cryptomare studies rely on identifying basalt-excavating dark-haloed craters [1,2].

Fresh basalts are often identified using spectral studies [e.g., 2, 3]. Individual spectra are extracted from pixels of interest, but with millions of data pixels in a study area, this can be time consuming. Users must choose which pixels to consider, thus the best spectra may not be found and spectrally interesting areas that are otherwise indistinct, may be overlooked.

So motivated, we developed an empirical technique for identifying fresh basalt spectra in Clementine data.

Study Area: Our study area is the region west of Mare Humorum (Figure 1). Previous work in this area [2, 4] provides a good reference for judging the accuracy of our results. The data consists of full resolution (303.23 pixels/km) Clementine UVVIS multispectral data and Lunar Orbiter (LO) photographic image data (512 pixels/km), downloaded from [5]. Weight% FeO values [5] were calculated from the Clementine data.

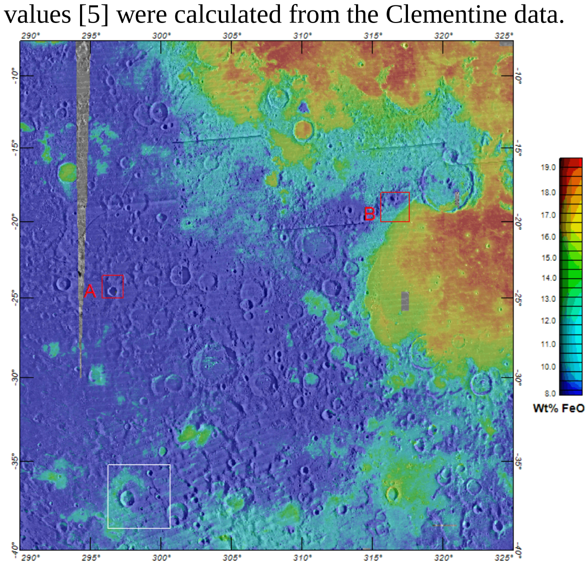

Figure 1: LO Image of the Humorum study area, with Lucey Iron [6] overlay. Red boxes show locations of the two training areas (Figure 4). White box gives location of Figure 5.

Method: In Clementine data, fresh basalt spectra have specific characteristics (Figure 2). Segment A has a positive slope. Segment B has a negative slope, contributing to an obvious band depth. The transition between segments B, C, and D is smoothly curved.

To quantify significant parameters for fresh basalt spectra, we selected two vastly different training sets (locations shown in Fig 1). Training set A is located in highland with relatively low iron content throughout. Training set B contains a mare/highland boundary and has a large range of iron values.

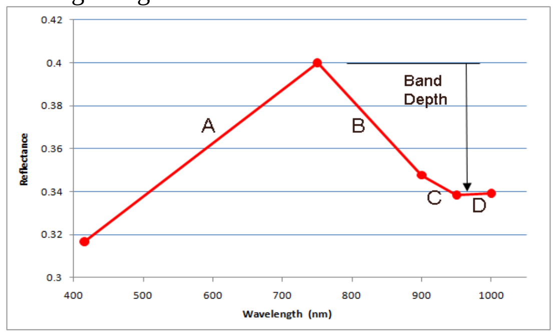

Figure 2: Ideal basalt spectra showing band depth, placement of the 4 segments, and the model relationship between segments B, C, and D.

Two apriori assumptions were made: 1) Band depth should be high, to correspond to fresh materials and for easier identification, 2) Segment B slope must be negative, since positive B slopes indicate highland spectra.

Band depth is quantified as (R750 – R950)/(R750-R415), where R750 is the 750 nm band reflectance, etc. For the initial training, only spectra with band depth >= 0.2 were considered. This resulted in 17,000 spectra, which were normalized and plotted, then visually analyzed to identify fresh basalt spectra.

Visual sorting can be subjective Figure 3 shows spectra ranging from ideal basalt to “non-basalt”. Ideal and “non-basalt” spectra are easily classified. However, the boundary between these is less clear. This ambiguity makes consistency in visual sorting challenging. Our choice of a large training set attempts to compensate for this ambiguity with statistics of large numbers.

From our starting set of 17000 spectra, we identified over 13,000 basalt spectra. Their locations are plotted in Figure 4.

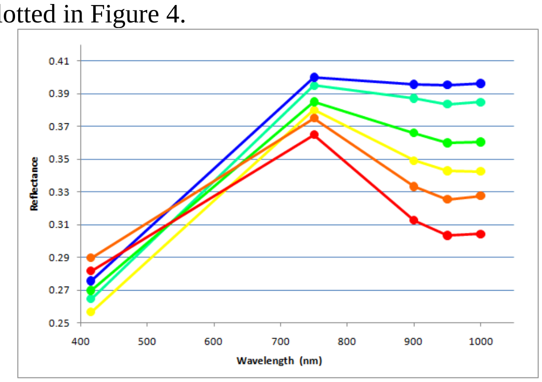

Figure 3: Suite of normalized spectra, offset from each other by 0.005, ranging from ideal basalt to “non-basalt” spectra.

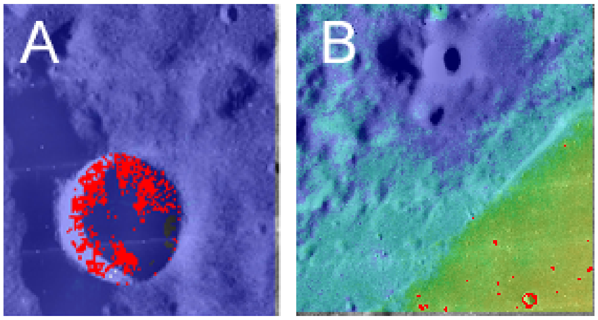

Figure 4: Training areas showing LO data with Lucey Iron overlay, and identified basalt spectra locations in red.

Analysis: Classified spectra were analyzed to find characteristics common to basalt spectra, but absent in "non-basalt" spectra. We focused on quantifying relationships between the slopes of segments B, C, and D.

Our 17,000 training spectra are modeled well by the first 2 parameters and bounds in Table 1. Application of these parameters results in 1173 false positives and 437 false negatives (an error rate of roughly 10%). False positives (spectra incorrectly identified as basalts) tend to fall in the ambiguous range between ideal and "non-basalt" spectra and so may have been misclassified in training. False negatives (spectra incorrectly classified as "non-basalts") are much less ambiguous. Therefore, these parameters should give conservative estimates for the presence of fresh basalts.

Table 1: List of empirical parameters and their max/min boundaries, used for identifying fresh basalt spectra in the Humorum study region.

Parameter	Equation	Min Value	Max Value
BC Angle	$\frac{3(R950-R900)}{(R900-R750)}$	-0.22	1.36
CD Angle	R1000-2R950-R900	0.0022	0.025
B Slope	$\frac{(R900-R750)}{3}$	-	-0.0025
Band Depth	$\frac{(R750-R950)}{(R750-R415)}$	0.1	-

To fine tune our algorithm, we applied the first 2 parameters of Table 1 to the entire 574,402 point training data set. Spectra identified as basalts by the algorithm were selectively surveyed and visually analyzed. Determining where basalt spectra can be realistic identified refined the bounds for the last 2 parameters.

Results: The parameters of Table 1 were applied to the entire Mare Humorum full resolution Clementine UVVIS data set. The results are encouraging. For the training areas, full run and training run results are self-consistent; the full run found all basalt regions identified in training, and no new regions. Identified basalt spectra generally correspond to regions of high topographic slope, where fresh basalts may be exposed by mass wasting. Furthermore, the locations of identified basalts, and their absence, correlates well with our previous work in this region [5].

There is significant potential for using these results in future work. In Figure 5, several previously unidentified dark-haloed craters are highlighted by basalt spectra (yellow dots). Incipient dark-haloed craters (no iron signature in ejecta, but basalts on their slopes) are also identified. On one crater, streaks of basalt spectra on the outside flank (white arrow) suggest recent freshening, possibly due to a landslide or a boulder rolling down slope. We envision using such results for future cryptomare and mare thickness analyses, as well as the study of other interesting phenomena that may be revealed by this technique.

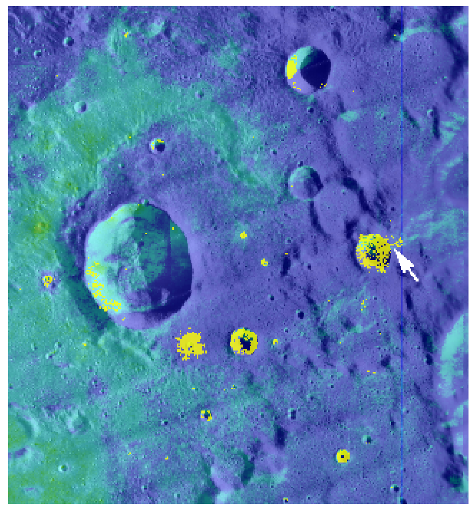

Figure 5: Area in white box from Figure 1, with locations of basalt spectra (identified by Table 1 algorithm) shown in yellow. White arrow shows location of possible landslide.

Conclusions: We developed a simple empirical method for identifying fresh basalt spectra in Clementine lunar data. This method works well in the Humorum area of the Moon, identifying basalt spectra on the slopes of basalt-containing craters. Application to other areas of the Moon remains to be tested.

Similar methods could be developed for the M3 and LRO data sets, when they are made available.

References: [1] Schultz P.H. and Spudis P.D. (1979) *Proc. LPSC 10th*, 2899-2918. [2] Antonenko I. (1999) *Volumes of Cryptomafic Deposits on the W. Limb of the Moon: Implications for Lunar Volcanism* (Thesis), Brown U. Providence, R.I. p305. [3] Tompkins S. and Pieters C.M. (1999) *Meteoritics & Planet. Sci., 34,* 25-41. [4] Antonenko I. and Osinski G.R. (2009) *Eos Trans. AGU, 90(22), Jt. Assem. Suppl.*, Abstract P31B-04. [5] UGGS Map-A-Planet, http://www.mapaplanet.org/explorer/moon.html. [6] Lucey P.G. *et al.* (2000) *J.G.R.*., 105, 20,297.